JACS
JOURNAL OF THE AMERICAN CHEMICAL SOCIETY
Communication
pubs.acs.org/JACS

Ultrasmall Sub-10 nm Near-Infrared Fluorescent Mesoporous Silica Nanoparticles

Kai Ma, Hiroaki Sai, and Ulrich Wiesner*

Department of Materials Science and Engineering, Cornell University, Ithaca, New York 14850, United States

Supporting Information

ABSTRACT: Ultrasmall sub-10 nm nanoprobes and carriers are of significant interest due to their favorable biodistribution characteristics in *in vivo* experiments. Here we describe the one-pot synthesis of PEGylated mesoporous silica nanoparticles with a single pore, tunable sizes around 9 nm and narrow size distributions that can be labeled with near-infrared dye Cy5.5. Particles are characterized by a combination of transmission electron microscopy, dynamic light scattering, fluorescence correlation spectroscopy, optical spectroscopy, nuclear magnetic resonance spectroscopy, and nitrogen sorption/desorption measurements. The possibility to distinguish an "inside" and "outside" may render these particles an interesting subject for further studies in sensing, drug delivery, and theranostics applications.

Cancer has become a leading cause of death worldwide, accounting for over 7.5 million deaths in 2008.[1] While one of the most important forms of cancer treatment, chemotherapeutic drugs often also kill healthy cells and cause toxicity to the patient. In the search for improved alternatives, nanocarriers have become an emerging platform for cancer therapy enabling drug delivery specifically into tumors.[2,3] Beginning in the mid-1980s, several types of targeting nanocarriers, based on polymer−protein conjugates and lipids, have successfully reached clinical trials.[4−10] However, there are still many challenges remaining, including rapid clearance, burst drug release and nonspecific uptake.[2] In order to overcome these challenges, nanocarriers with better properties need to be designed.[3] A promising alternative material to polymers is mesoporous silica due to its high-surface area, stability, and biocompatibility. Surface-functionalized mesoporous silica nanoparticles (MSNs) can deliver multiple types of cargo, such as DNA, drug molecules, or even quantum dots, into cells and tissues of plants or animals.[11−22] However in the current state of development, such MSN-based nanocarriers have not yet reached clinical trials. One of the reasons is that silica typically needs a fairly long time to dissolve under physiological conditions, resulting in potential particle accumulation in the body, which may in turn cause long-term toxicity.[2] Even in cases where MSNs dissolve quite rapidly,[22] questions about the dissolution mechanism, biodistribution, and toxicity remain.

One way to overcome these problems is to design nanocarriers with sizes smaller than 10 nm, i.e., below what is believed to be the threshold for renal clearance.[23] To this end, we recently developed fluorescent core−shell silica nanoparticles referred to as Cornell dots or simply C dots.[24−26] Synthesized to sizes below 10 nm, PEGylated C dots show efficient renal clearance in animals.[27] Carrying cyclic arginine-glycine-aspartic acid (cRGD) peptide ligands as well as radioiodine, an ultrasmall cancer-targeted dual-modality (optical and positron emission tomography, PET) C dot probe for melanoma was indeed recently approved for a first in-human clinical trial.[28]

In order to endow such ultrasmall silica nanoparticles with additional, e.g., therapeutic, properties for clinical applications, it is desirable to develop mesoporous particles with sizes smaller than 10 nm. Although recently the size of MSNs has been pushed down to less than 20 nm,[29,30] the synthesis of fluorescent MSNs smaller than 10 nm and with narrow particle size distributions still remains a challenge.

We present a one-pot synthesis of PEGylated MSNs with sizes precisely tunable around 9 nm (Figure 1) that have narrow particle size distributions and a single pore and can be labeled with near-infrared (NIR) dye Cy5.5. Keys for the successful synthesis of such ultrasmall MSNs are (i) fast hydrolysis of the silica (silane) precursors, (ii) slow silica condensation/particle growth, and (iii) particle growth

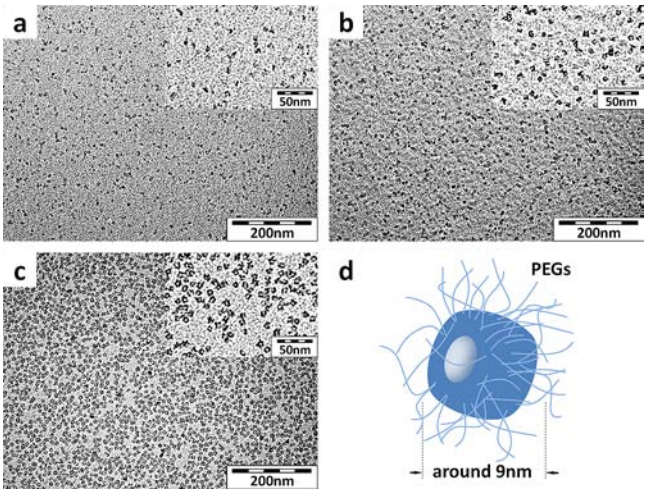

Figure 1. TEM images of silica particles with different diameters: (a) 6.6, (b) 8.2, and (c) 9.3 nm. Inserts display images of the same samples but at higher magnification. (d) Schematic of a single-pore MSN coated with PEG chains.

Received: May 22, 2012
Published: July 25, 2012

   dx.doi.org/10.1021/ja3049783 | J. Am. Chem. Soc. 2012, 134, 13180−13183

termination via the addition of PEG-silane quenching further silica condensation on the particle surface.

As detailed in the Supporting Information (SI), particle synthesis was performed near room temperature (30 °C) in aqueous solution in the presence of hexadecyltrimethyl ammonium bromide (CTAB) as structure directing agent, with tetramethyl orthosilicate (TMOS) as silica source, and ammonium hydroxide as base catalyst. PEG-silane was added directly into the synthesis batch to quench particle formation. A postsynthesis heating step and subsequent solution workup, including acid extraction of CTAB via dialysis, provided the final particles.

While tetraethyl orthosilicate (TEOS) is commonly used in the synthesis of MSNs, here TMOS was chosen as the silica source.[30] The hydrolysis rate of TMOS is much faster than that of TEOS, and its solubility in water is higher. As a result, instead of forming a second oil phase and gradually hydrolyzing at the oil droplet–water interface, as is the case for TEOS,[29,31] TMOS directly dissolves in water and hydrolyzes once added into the reaction. An accelerated completion of the hydrolysis process helps initiating/nucleating more MSN growth in the presence of CTAB micelles over a smaller period of time thus leading to smaller particles and better control over particle size distribution. Lowering the condensation rate by moving to near room temperature conditions or lowering the concentration of TMOS and CTAB results in slower particle growth and smaller particles. By carefully optimizing the system, we found conditions where the particles grow from around 2 nm to sizes larger than 10 nm within a convenient time window. Particle growth is terminated by quenching further condensation on the particle surface through addition of PEG-silane. A final heat treatment at 80 °C at the end of the synthesis improves particle stability. Through the PEGylation step as part of the one-pot synthesis the resulting sub-10 nm MSNs are already sterically stabilized, a prerequisite for working in many biological environments.[32,33]

In order to demonstrate the kind of particle size and size distribution control achievable by this approach, Figure 1a–c shows transmission electron microscopy (TEM) results on particles from three synthesis batches obtained from varying synthesis conditions (see Table S1, SI) leading to increasing particle size in the direction from a–c. The smaller magnification images illustrate the high degree of homogeneity in particle size, while the higher resolution images in the insets reveal details of particle structure. In all cases TEM results suggest that silica has grown around an individual pore formed by CTAB template. An illustration of this type of structure, including the PEG chains on the outside of the particles, is depicted in Figure 1d. While in Figure 1a single pore particle formation is largely incomplete, Figure 1b already displays side-on as well as head-on particles. Particles in Figure 1c exhibit the most well-defined structure (additional particle images in SI). Figure 2a shows results of three independent size measurements for each of the three particle batches by dynamic light scattering (DLS). The data sets are very consistent and provide average hydrodynamic diameters of 6.6, 8.2, and 9.3 nm for particles in Figure 1a–c, respectively. Alternatively, we determined particle size and size distribution by quantitative TEM image analysis (details in SI). TEM average diameters from data in Figure 2b are 5.7, 7.3, and 8.9 nm, i.e., slightly smaller than from DLS. Both DLS and TEM results reveal fairly narrow size distributions and absence of any significant aggregation behavior. Smaller average diameters from TEM

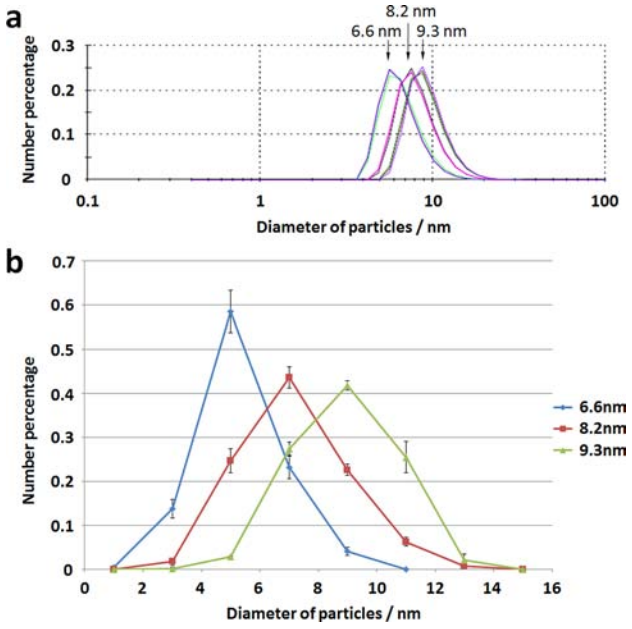

Figure 2. Size distribution of particles determined by (a) DLS and (b) TEM image analysis. In DLS each data set was measured three times per batch.

are expected, as this technique, in contrast to DLS, is insensitive to the PEG layer and water molecules dragged with it. As a result in the following we will use DLS diameters as descriptors of the different particles.

TEM images also allowed analyzing the distribution of the number of pores per particle. As shown in Figure 3, for around

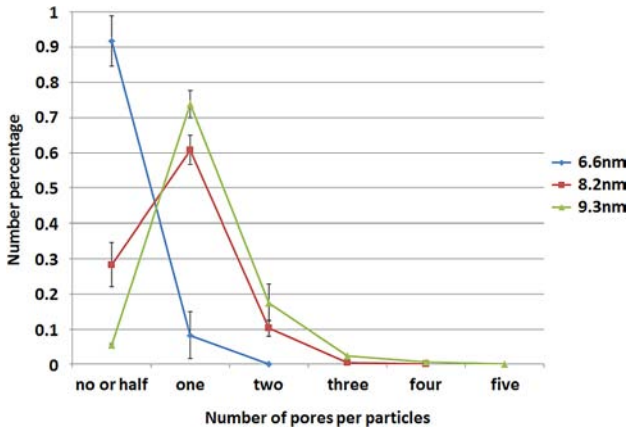

Figure 3. Distribution of number of pores per particle as determined from TEM image analysis; each data point is obtained by averaging three independent analyses.

90% of the 6.6 nm particles single-pore particle formation is incomplete (referred to as "no or half" pore particles in Figure 3). As the diameter increases to 8.2 nm, the percentage of incomplete single-pore particles significantly drops from around 90% to below 30%. Increasing the diameter to 9.3 nm finally results in a fairly narrow distribution of the number of pores per particle in which more than 70% are single-pore particles. This distribution already is quite symmetric. Further increasing particle size most likely would bias the distribution toward an increase in the number of particles with more than one pore. We therefore speculate that the optimized hydrodynamic

dx.doi.org/10.1021/ja3049783 | J. Am. Chem. Soc. 2012, 134, 13180–13183

particle diameter for achieving single-pore particles in our synthesis should be close to the 9.3 nm value of the third synthesis batch.

Particles were further characterized by liquid ^{1}H NMR to demonstrate successful CTAB removal by acetic acid extraction and the presence of PEG chains on the particle surface (details in SI). In order to independently confirm TEM results on the pore structure we performed nitrogen sorption/desorption measurements on the 9.3 nm particles (see SI). While such measurements are challenging because of the presence of the PEG chains, working with plasma-treated sample batches clearly confirmed the existence of well-defined pores with sizes between 2.8 and 3 nm, depending on the plasma treatment duration.

In order to visualize such <10 nm sized single-pore silica nanoparticles, in particular in biological environments, labeling with NIR dyes is highly desirable.[28,34] To this end we slightly modified the synthesis protocol for the 9.3 nm particles by simultaneously adding silane conjugated Cy5.5 and TMOS into the reaction mixture (details in SI). We will refer to these dye-labeled mesoporous silica nanoparticles as mC dots. Cy5.5 has absorption and emission maxima around 675 and 700 nm, respectively, thus limiting interference from background fluorescence in biological tissue.[34] Adding Cy5.5-silane conjugate to the reaction left the particle architecture largely unchanged. The DLS derived average hydrodynamic diameter of this sample increased to 9.6 nm as compared to 9.3 nm for the unlabeled particle (Figure 4a). Furthermore, most of the particles still showed single-pore architecture (Figure 4c). In order to verify that these particles carry a fluorescent label we used fluorescent correlation spectroscopy (FCS) for further particle characterization (Figure 4b). This technique is similar to DLS but uses the fluorescence of the diffusing moiety rather than the scattered light to generate autocorrelation data. Figure 4b compares FCS results from free Cy5.5 dye and Cy5.5 labeled single-pore silica nanoparticles. As expected for the slower diffusing particle, its curve is shifted to longer times. From the correlation time hydrodynamic diameters can be derived.[26] They are 1.5 and 10.2 nm for free dye and particle, respectively. FCS may thus slightly bias the true particle distribution to larger sizes as not every particle may carry a dye. It should be noted, however, that the differences are rather small (10.2 nm from FCS vs 9.6 nm from DLS). As explained in detail in a previous publication,[26] from the amplitude $G(0)$ of the FCS autocorrelation one can derive the dye/particle concentration in solution, while the optical detector count rate per diffusing species provides a direct measure of its brightness. Furthermore, in combination with static optical and fluorescence spectroscopy, FCS helps to provide information about number of dyes per particle and per dye enhancement over free dye in aqueous solution as well as particle brightness (details in SI). From analysis of spectrophotometer and spectrofluorometer data in combination with FCS concentration information on the free dye and particles, there are around 2.6 Cy5.5 dyes in one particle, and the quantum enhancement of the Cy5.5 dye in the particles versus in aqueous solution is around 1.3 (Figure S3). Thus a Cy5.5-doped mC dot is around 3.4 times brighter than a free Cy5.5 dye. This is consistent with direct brightness comparisons from FCS optical detector count rates (Table S3). It is further consistent with results of equivalent measurements on Cy5 containing ~7 nm C dots.[28] Considering that just conjugation to a silane alone can already have a positive effect on the brightness of Cy dyes,[34] this analysis remains inconclusive on whether in the present case the Cy5.5 dyes are fully incorporated inside the silica walls or whether they sit at or on the silica surface of the mC dots. Since the final PEG-silane treatment is expected to cover the particle surface with an additional silica surface layer, the latter is unlikely.

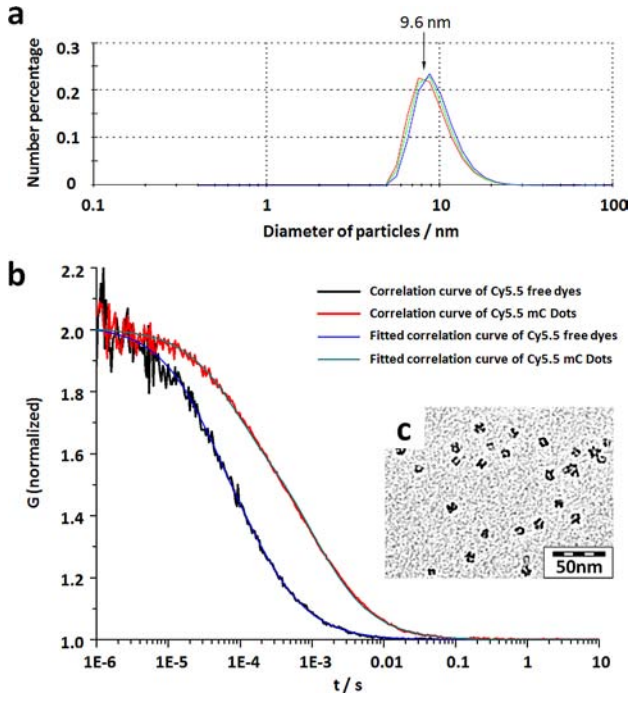

Figure 4. Characterization of Cy5.5 labeled mC dots. (a) DLS size measurements. (b) Normalized FCS curves for Cy5.5 free dye (black and blue lines) and Cy5.5 containing mC dots (red and green lines). (c) TEM image of the Cy5.5 mC dots.

It is interesting to note that the single-pore silica nanoparticles described here have an "inside" and an "outside". As has been shown by others, inside and outside surfaces of such materials can be distinguished when additional conjugation chemistry is desired, e.g., to bind targeting or pharmaceutical moieties.[35] For example, during the PEGylation process the particle pores are occupied by structure directing CTAB molecules. Therefore, in contrast to the outer silica surface, it is expected that the PEG-silane coating has a significantly diminished probability of attaching to the (inside) surface of the pores. After CTAB extraction the unoccupied inside of the pore walls thus can be used for additional silane chemistry to conjugate specific moieties, which could be complementary to what is used on the outside of the PEGchains. Being in a similar size regime, it is this ability to distinguish between the inside and the outside, and the larger overall surface area available for conjugation chemistry, which distinguishes these single-pore silica nanoparticles (or mC dots) from conventional C dots. Future work may demonstrate how this feature can be used as an advantage in areas like sensing, drug delivery, and theranostics.

■ ASSOCIATED CONTENT

Ⓢ Supporting Information

Detailed synthesis protocols and characterization methods are provided. This material is available free of charge via the Internet at http://pubs.acs.org.

AUTHOR INFORMATION

Corresponding Author

ubw1@cornell.edu

Notes

The authors declare no competing financial interest.

ACKNOWLEDGMENTS

K.M. acknowledges National Science Foundation (NSF) for financial support (grant MPS/DMR-1008125). H.S. acknowledges financial support from the National Science Foundation (NSF) Single Investigator Award (grant DMR-1104773). The authors acknowledge the Cornell Center for Materials Research (CCMR) and the Nanobiotechnology Center (NBTC) of Cornell University for the use of facilities. The authors also gratefully acknowledge S. K. Iyer, J. Drewes, Y. Sun, and Z. Li of Cornell University and Dr. T. Suteewong of Memorial Sloan-Kettering Cancer for helpful discussions and kind experiment assistance.

REFERENCES

(1) *Globocan 2008*; *IARC*: France, 2010.

(2) Peer, D.; Karp, J. M.; Hong, S.; Farokhzad, O. C.; Margalit, R.; Langer, R. *Nat. Nanotechnol.* **2007**, *2*, 751−760.

(3) Schroeder, A.; Heller, D. A.; Winslow, M. M.; Dahlman, J. E.; Pratt, G. W.; Langer, R.; Jacks, T.; Anderson, D. G. *Nat. Rev. Cancer* **2012**, *12*, 39−50.

(4) Couvreur, P.; Kante, B.; Grislain, L.; Roland, M.; Speiser, P. *J. Pharm. Sci.* **1982**, *71*, 790−792.

(5) Batrakova, E. V.; Dorodnych, T. Y.; Klinskii, E. Y.; Kliushnenkova, E. N.; Shemchukova, O. B.; Goncharova, O. N.; Arjakov, S. A.; Alakhov, V. Y.; Kabanov, A. V. *J. Cancer* **1996**, *74*, 1545−1552.

(6) Tolcher, A. W.; Sugarman, S.; Gelmon, K. A.; Cohen, R.; Saleh, M.; Isaacs, C.; Young, L; Healey, D.; Onetto, N.; Slichenmyer, W. *J. Clin. Oncology* **1999**, *17*, 478−484.

(7) Nakanishi, T.; Fukushima, S.; Okamoto, K.; Suzuki, M.; Matsumura, Y.; Yokoyama, M.; Okano, T.; Sakurai, Y.; Kataoka, K. *J. Controlled Release* **2001**, *74*, 295−302.

(8) Torchilin, V. P. *Nat. Rev. Drug Discovery* **2005**, *4*, 145−160.

(9) Duncan, R. *Nat. Rev. Cancer* **2006**, *6*, 688−701.

(10) Torchilin, V. P. *Pharm. Perspect. Pharm. Res.* **2007**, *24*, 1−16.

(11) Luo, D.; Saltzman, W. M. *Nat. Biotechnol.* **2000**, *18*, 893−895.

(12) Radu, D. R.; Lai, C. Y.; Jeftinija, K.; Rowe, E. W.; Jeftinija, S.; Lin, V. S. Y. *J. Am. Chem. Soc.* **2004**, *126*, 13216−13217.

(13) Vivero-Escoto, J. L.; Slowing, I. i.; Trewyn, B. G.; Lin, V. S. Y. *Small* **2010**, *6*, 1952−1967.

(14) Rosenholm, J. M.; Peuhu, E; Eriksson, J. E.; Sahlgren, C.; Linden, M. *Nano let.* **2009**, *9*, 3308−3331.

(15) Du, L.; Liao, S.; Khatib, H. A.; Stoddart, J. F.; Zink, J. I. *J. Am. Chem. Soc.* **2009**, *131*, 15136−15142.

(16) Bharali, D. J.; Klejbor, I.; Stachowiak, E. K.; Dutta, P.; Roy, I.; Kaur, N.; Bergey, E. J.; Prasad, P. N.; Stachowiak, M. K. *Proc. Natl Acad. Sci. U.S.A.* **2005**, *102*, 11539−11544.

(17) Hu, S.; Liu, T.; Huang, H.; Liu, D.; Chen, S. *Langmuir* **2008**, *24*, 239−244.

(18) Roy, I.; Ohulchanskyy, T. Y.; Bharali, D. J.; Pudavar, H. E.; Mistretta, R. A; Kaur, N.; Prasad, P. N. *Proc. Natl Acad. Sci. U.S.A.* **2005**, *102*, 279−284.

(19) Lee, J. E.; Lee, N.; Kin, T.; Kim, J.; Hyeon, T. *Acc. Chem. Res.* **2011**, *44*, 893−902.

(20) Torney, F.; Trewyn, B. G.; Lin, V. S. L.; Wang, K. *Nat. Nanotechnol.* **2007**, *2*, 295−300.

(21) Piao, Y.; Burns, A.; Kim, J.; Wiesner, U.; Hyeon, T. *Adv. Funct. Mater.* **2008**, *18*, 3745−3758.

(22) Ashley, C. E.; Carnes, E. C.; Phillips, G. K.; Padilla, D.; Durfee, P. N.; Brown, P. A.; Hanna, T. N.; Liu, J.; Phillips, B.; Carter, M. B.; Carroll, N. J.; Jiang, X.; Dunphy, D. R.; Willman, C. L.; Petsev, D. N.; Evans, D. G.; Parikh, A. N.; Chackerian, B.; Wharton, W.; Peabody, D. S.; Brinker, C. F. *Nat. Mater.* **2011**, *10*, 389−397.

(23) Choi, H. S.; Liu, W.; Misra, P.; Tanaka, E.; Zimmer, J. P.; Ipe, B. I.; Bawendi, M. G.; Frangioni, J. V. *Nat. Nanotechnol.* **2007**, *25*, 1165−1170.

(24) Ow, H.; Larson, D.; Srivastava, M.; Baird, B.; Webb., W.; Wiesner, U. *Nano Lett.* **2005**, *5*, 113−117.

(25) Burns, A.; Ow, H.; Wiesner, U. *Chem. Soc. Rev.* **2006**, *35*, 1028−1042.

(26) Larson, D. R.; Ow, H.; Vishwasrao, H. D.; Heikal, A. A.; Wiesner, U.; Webb, W. W. *Chem. Mater.* **2008**, *20*, 2677−2684.

(27) Burns, A.; Vider, J.; Ow, H.; Herz, E.; Penate-Medina, O.; Baumgart, M.; Larson, S. M.; Wiesner, U.; Bradbury, M. *Nano Lett.* **2009**, *9*, 442−448.

(28) P., B.; Schaer, D.; Ow, H.; Burns, A.; DeStanchina, E.; Longo, V.; Herz, E.; Iyer, S.; Wolchok, J.; Larson, S. M.; Wiesner, U.; Bradbury, M. *J. Clin. Invest.* **2011**, *121*, 2768−2780.

(29) Lu, F.; Wu, S.; Hung, Y.; Mou, C. *Small* **2009**, *5*, 1408−1413.

(30) Urata, C.; Aoyama, Y.; Tonegawa, A.; Yamauchi, Y.; Kuroda, K. *Chem. Commun.* **2009**, 5094−5096.

(31) Wang, J.; Sugawara-Narutaki, A.; Fukao, M.; Yokoi, T.; Shimojima, A.; Okubo, T. *ACS Appl. Mater. Interfaces* **2011**, *3*, 1538−1544.

(32) Lin, Y.; Abadeer, N.; Haynes, C. L. *Chem. Commun.* **2011**, *47*, 532−534.

(33) Lin, Y.; Haynes, C. L. *J. Am. Chem. Soc.* **2010**, *132*, 4834−4842.

(34) Herz, E.; Ow, H.; Bonner, D.; Burns, A.; Wiesner, U. *J. Mater. Chem.* **2009**, *19*, 6341−6347.

(35) Slowing, I. I.; Vivero-Escoto, J. L.; Wu, C. W.; Lin, V. S. Y. *Adv. Drug Delivery Rev.* **2008**, *60*, 1278−1288.